IEEE Access
Multidisciplinary | Rapid Review | Open Access Journal

Received 30 April 2024, accepted 23 May 2024, date of publication 28 May 2024, date of current version 7 June 2024.

Digital Object Identifier 10.1109/ACCESS.2024.3406857

RESEARCH ARTICLE

Improving Insertion Loss of Sonic Crystal Active Noise Barrier by Reinforcement Learning and Finite Difference Time Domain Simulations

DAVID RAMÍREZ-SOLANA[1,2], JAIME GALIANA-NIEVES[2], JAVIER REDONDO[2], AGOSTINO MARCELLO MANGINI[1], (Senior Member, IEEE), AND MARIA PIA FANTI[1], (Fellow, IEEE)

[1]Dipartimento di Ingegneria Elettrica e dell'Informazione, Politecnico di Bari, 70125 Bari, Italy
[2]Instituto de Investigación para la Gestión Integrada de Zonas Costeras, Universitat Politècnica de València, Campus de Gandía, 46730 Gandia, Spain

Corresponding author: David Ramírez-Solana (david.ramirezsolana@poliba.it)

This work was supported in part by the Spanish "Ministerio de Ciencia e Innovación" and "Agencia Estatal de Investigación" of Spain through project MCIN/AEI/10.13039/501100011033 under Grant PID2021-124908NB-I00, and in part by the European Regional Development Fund (ERDF) A way of making Europe.

ABSTRACT Sonic crystal noise barriers (SCNB) have emerged as a promising solution for mitigating traffic noise pollution. These barriers utilize periodic structures to selectively reflect acoustic waves at specific target frequencies, offering the advantage of being permeable to light and wind. However, their installation and maintenance costs have hindered widespread adoption. In contrast, active noise control (ANC) systems leverage speakers and microphones to generate opposing sound waves that cancel out incoming noise, presenting a potentially cost-effective alternative. The efficacy of ANC, however, hinges on the precision of noise prediction models and control algorithms. Reinforcement Learning (RL) technique, an interdisciplinary area of machine learning, has shown promise in enhancing ANC systems by enabling them to adapt to changing noise conditions and achieve superior noise reduction, particularly in enclosed spaces. Despite these advancements, several challenges remain in applying RL to ANC systems for SCNB. This paper explores these challenges and proposes an RL-based solution for autonomous ANC systems within the context of SCNB, utilizing a Finite Difference Time Domain (FDTD) simulation environment to address low-frequency, moving sources, and outdoor propagation noise scenarios.

INDEX TERMS Reinforcement learning, noise barriers, finite-difference time-domain, sonic crystals.

I. INTRODUCTION

The use of metamaterials in industrial applications has been promising during the last decade [1], [2], [3]. In the field of noise barriers, Sonic Crystal Noise Barriers (SCNB) represent an innovative approach to mitigate the pervasive issue of traffic noise pollution. These barriers are designed to selectively target and attenuate sound waves at specific frequencies through the use of periodic structures, a concept rooted in the science of sonic crystals (SC) [4]. By carefully designing the topology of scatterers or adjusting the lattice constant between them, engineers can create SCNB suitable to reduce noise pollution effectively. The SCNB have the property of allowing the passage of wind and light [5], [6]. This advantage makes them more aesthetically pleasing and environmentally friendly than traditional noise barriers, usually built using solid structures made with opaque materials such as concrete or wooden planks [5], [6]. However, the substantial costs associated with the installation and maintenance of SCNB have limited their widespread implementation [7].

Contrary to that, Active Noise Control (ANC) systems offer a potentially cost-effective approach to noise reduction. These systems operate by using strategically placed microphones to capture incoming noise and speakers to emit sound waves that are precisely out of phase with the noise, leading to cancellation [8]. ANC has been successfully applied in various domains, such as automotive [9], [10] and industrial settings [11], where reducing noise is crucial. However, the

The associate editor coordinating the review of this manuscript and approving it for publication was Qingchun Chen.

effectiveness of ANC systems relies heavily on the accuracy of noise prediction models and the sophistication of the control algorithms used to generate the anti-phase sound waves [12].

The idea of improving the insulation of noise barriers employing ANC systems has been applied to traditional barriers since several decades [13]. Some of the studies are applied to real cases [14], other ones have developed their own experimental validations in anechoic chambers [15] and exploiting unidirectional sources [16].

Control algorithms play a pivotal role in ANC systems, and one approach that has gained prominence in recent years is Reinforcement Learning (RL) [17]. RL is a subfield of Machine Learning (ML) that focuses on developing algorithms capable of learning optimal actions through interaction with an environment and feedback in the form of rewards [18]. There is a wide scope of applications that have demonstrated its efficiency optimizing its processes such as Blockchain [19] or additive manufacturing processes [20].

Deep Q-learning and actor-critic methods, two prominent branches of RL, have been applied successfully to ANC systems [21], enabling them to adapt dynamically to changing noise conditions and improve noise reduction performance, especially in enclosed spaces or noise signals without simulations [22]. In Table 1, some of the most representative works concerning the principal components of this study are presented. More precisely, Table 1 compares works involving noise barriers (NB), with or without SC, as well as ANC works categorized as either RL based or non-RL-based.

Before delving into the proposed RL-based solution for integrating ANC with SCNB, it is essential to recognize the important challenges and considerations that arise when combining these two technologies.

The SCNB challenges are the following:

- **Low-Frequency Performance:** SCNB, despite their effectiveness at certain frequencies, often struggle to attenuate low-frequency noise effectively. This limitation is particularly relevant in cases where the width of the barrier should not exceed a certain value [23].
- **Normal Incidence Insulation:** Many SCNB studies focus on noise reduction at normal incidence, neglecting the real-world scenario of random incidence noise sources. This limited normal incidence approach can differ from the noise reduction performance when the noise source is not aligned with the barrier [24].
- **Plane Wave Excitation:** SCNB designs frequently relies on the assumption of an incident plane wave as the primary noise source [25]. That means that the source is located far enough away, but that condition is usually not satisfied.

In addition, the ANC challenges are the following:

- **Fixed Primary Noise Sources:** Traditional ANC systems are primarily designed for scenarios where the primary noise source is fixed and known. In contrast, outdoor environments with varying noise sources pose unique challenges, as identifying and tracking these sources in real-time is complex.
- **Enclosed Spaces:** Most existing ANC applications target enclosed spaces [26], such as closed rooms, or ducts. The extension of ANC to outdoor environments with open boundaries and complex propagation conditions needs a different approach.

TABLE 1. Noise mitigation solutions review.

Name	Year	SC	NB	ANC	RL
Ise et al.[13]	1991	-	X	X	-
Lang et al.[34]	1993	-	X	X	-
Guo and Pan[15]	1998	-	X	X	-
Sánchez-Pérez et al.[4]	2002	X	X	-	-
Chen et al.[16]	2011	-	X	X	-
Sánchez-Dehesa et al.[35]	2011	X	X	-	-
Raeisy et al.[36]	2013	-	-	X	X
Castiñeira-Ibáñez et al.[37]	2015	X	X	-	-
Morandi et al.[38]	2016	X	X	-	-
Hoseini Sabzevari et al.[22]	2017	-	-	X	X
Aslan and Paurobally[26]	2018	-	-	X	-
Wang et al.[39]	2018				X
Sohrabi et al.[14]	2020	-	X	X	-
Latifi et al.[40]	2020				X
Mohapatra and Jena[41]	2021	X	X	-	-
Kurowski and Kostek[33]	2021				X
Jabeen et al.[12]	2021	-	-	X	-
Qin et al.[42]	2022	X	X	-	-
Kim and Altinsoy[9]	2022	-	-	X	-
D'orazio et al.[43]	2023	X	X	-	-
Mori et al.[10]	2023	-	-	X	-
Redondo et al.[44]	2023	X	X	-	-
Sohrabi et al.[45]	2023	-	X	X	-
Lu et al.[11]	2023	-	-	X	-
Ramírez-Solana et al.[46]	2024	X	X	-	-

To overcome these challenges and bridge the gap between SCNB and ANC, this research proposes the development of an RL-based procedure for constructing SCNB that enhance their insulation performance by integrating an ANC system utilizing microphones and speakers. This approach leverages a Finite Difference Time Domain (FDTD) simulation environment handling low-frequency noise and dynamic outdoor noise propagation.

The FDTD method, initially introduced by Yee in 1966 [27] for investigating the scattering of electromagnetic waves, has found applications in various acoustic domains. A parallel approach suitable for acoustic purposes has emerged with success in different applications. These applications encompass but are not limited to sound diffusers [22], [23],

absorbing panels [30] and sonic crystal waveguides [31] and SCNB [32].

The FDTD modelling has proven beneficial in scenarios where spatial constraints and low-frequency bandwidth extension are critical considerations, and the FDTD simulation has also demonstrated its effectiveness in generating successful RL optimizations [33].

This approach offers several advantages:

- **Adaptation to Changing Conditions:** By continually learning and adjusting its control strategy, the RL-based ANC system can respond to varying noise sources, frequencies, and incidence angles, overcoming some of the limitations associated with traditional ANC.
- **Improved Low-Frequency Performance:** RL algorithms can learn sophisticated control strategies to tackle low-frequency noise, a known weakness of SCNB, by optimizing the placement and operation of ANC speakers.
- **Outdoor Noise Propagation Modelling:** The integration of a FDTD simulation environment allows for the more realistic modelling of outdoor noise propagation, to evaluate ANC effectiveness in open environments.

The paper is organized as follows. Section II presents the employed methodology to create the FDTD simulations and the set-up of the RL problem, Section III specifies the case study of RL applied to a SCNB with ANC system. Section IV presents the results of the training and deployment of the RL process and the acoustic analysis, and Section V encapsulates the conclusions and the future works.

II. METHODOLOGY

The tools and procedures to improve the SCNB with the ANC system are presented in this section. First, the steps followed for the implementation of the FDTD simulation method [47]. are described. Secondly, we explain the RL chosen agent procedure.

A. FINITE DIFFERENCE TIME DOMAIN SIMULATION TECHNIQUE

1) BASICS

The equations for momentum conservation and continuity provide the basis for an acoustic FDTD model without any sound sources. These models may be expressed as follows in a homogeneous medium with no losses:

$$\frac{\partial p}{\partial t} + k\vec{\nabla}\cdot\vec{u} = 0, \tag{1}$$

$$\vec{\nabla}p + \rho_0\frac{\partial \vec{u}}{\partial t} = 0, \tag{2}$$

where $\vec{u} = (u_x, u_y)$ is the vector denoting the particle velocity field, p represents the pressure field , ρ_0 stands for the mass density of the medium and $k = \rho_0 c^2$ is the compressibility of the medium. The central finite difference technique is used to approximate the spatial and temporal derivatives of pressure and particle velocity. For instance, we can use this method to estimate the derivative of sound pressure with respect to the x-coordinate, which can be expressed by the following equation:

$$\left.\frac{\partial p}{\partial x}\right|_{x=x_0} \approx \frac{p\left(x_0+\frac{\Delta x}{2}\right) - p\left(x_0-\frac{\Delta x}{2}\right)}{\Delta x}. \tag{3}$$

In particular, the spatial interval denoted by Δx represents the distance between closely-spaced points along the x-axis. In two dimensions, we must define three grids: one for pressure and two for the different components of particle velocity. To minimize the influence of higher-order terms in equations (4), (5) and (6), these grids are 'staggered'. For instance, the mesh for the x component of particle velocity is shifted by $\Delta x/2$ relative to the pressure mesh. The same principle applies to the time intervals; the particle velocity meshes are shifted by Δt/2 in time compared to the pressure mesh. By adopting this approach, we can derive a set of updated equations that allow us to determine the values of pressure and particle velocity after iterating for a specified number of steps. These equations are the following:

$$p_{i,j}^{n+1/2} = p_{i,j}^{n-1/2} - k\ \Delta t\left(\frac{ux_{i+1/2,j}^{n} - ux_{i-1/2,j}^{n}}{\Delta x} + \frac{uy_{i,j+1/2}^{n} - uy_{i,j-1/2}^{n}}{\Delta y}\right) \tag{4}$$

$$ux_{i+1/2,j}^{n+1} = ux_{i+1/2,j}^{n} - \frac{\Delta t}{\rho}\left(\frac{p_{i+1,j}^{n+1/2} - p_{i,j}^{n+1/2}}{\Delta x}\right) \tag{5}$$

$$uy_{i,j+1/2}^{n+1} = uy_{i,j+1/2}^{n} - \frac{\Delta t}{\rho}\left(\frac{p_{i,j+1}^{n+1/2} - p_{i,j}^{n+1/2}}{\Delta y}\right). \tag{6}$$

The superscripts denote the time index, and the subscripts denote the spatial indices as follows:

$$p_{i,j}^{n+1/2} = p(i\ \Delta x, j\ \Delta y, (n+1/2\ )\ \Delta t) \tag{7}$$

$$ux_{i+1/2,j}^{n} = u_x((i+1/2\ )\ \Delta x, j\ \Delta y, n\ \Delta t) \tag{8}$$

$$uy_{i,j+1/2}^{n} = u_y(i\ \Delta x, (j+1/2\ )\ \Delta y, n\ \Delta t). \tag{9}$$

To have a better understanding of the update equations, Fig. 1 represents the FDTD scheme.

With the aim of guaranteeing the numerical convergence, it is important that the time step is sufficiently small to accurately simulate wave propagation.

This relationship between the spatial steps and the time step is determined by the Courant number s, which can be defined as follows in two dimensions:

$$s = c\Delta t\sqrt{\left(\frac{1}{\Delta x}\right)^2 + \left(\frac{1}{\Delta y}\right)^2} \leq 1. \tag{10}$$

Another limitation of the FDTD method, which is shared with other numerical techniques, arises from the dependence of the maximum element size in discretization on the frequency. The standard criterion suggests using at least four elements per wavelength: in the related literature [48] it is shown that a high level of accuracy necessitates a minimum of 10 elements per wavelength. Consequently, at high

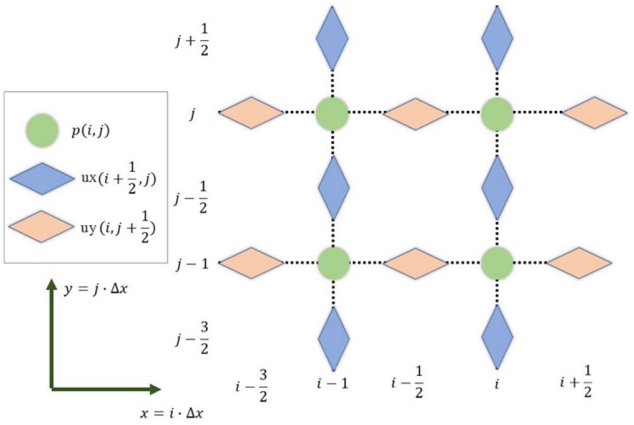

FIGURE 1. FDTD scheme of pressure and particle velocity fields.

frequencies, solving the numerical problem becomes computationally intensive. In this paper, we will employ a spatial step small enough to ensure accurate results up to 2kHz.

2) ABSORBING BOUNDARY CONDITIONS

In this study, to remove unwanted reflections from the boundaries of the computational domain, an absorbing boundary condition is used. The technique, known as "Perfectly Matched Layers" (PML) [49], [50], [51], [52], is chosen. PML introduces a lossy medium near the boundaries, requiring modifications to equations (1) and (2) to incorporate attenuation factors for each dimension considered (denoted as γ_x and γ_y in two dimensions). This adjustment is expressed as follows:

$$\frac{\partial p_x}{\partial t} + \gamma_x p_x + k\left(\frac{\partial u_x}{\partial x}\right) = 0 \tag{11}$$

$$\frac{\partial p_y}{\partial t} + \gamma_y p_y + k\left(\frac{\partial u_y}{\partial y}\right) = 0 \tag{12}$$

$$\frac{\partial p}{\partial x} + \rho\left(\frac{\partial u_x}{\partial t} + \gamma_x u_x\right) = 0 \tag{13}$$

$$\frac{\partial p}{\partial y} + \rho\left(\frac{\partial u_y}{\partial t} + \gamma_y u_y\right) = 0. \tag{14}$$

In equations (11)-(14) the sound pressure p is divided into two separate components p_x and p_y. These components do not have any physical significance and are defined merely for the purpose of optimizing the absorption performance. The attenuation factors are set to zero within the integration area but are heightened in regions near the boundaries.

B. REINFORCEMENT LEARNING

The RL technique is an interdisciplinary area of ML dedicated to the domain of sequential decision-making. It revolves around artificial agents that, akin to their biological counterparts, refine their capabilities through interactions with the surrounding environment. Leveraging experiential knowledge (States), the artificial agents strive to accomplish defined objectives, presented in the form of cumulative rewards as it is illustrated in Fig. 2. The essence of RL lies in the agent's capacity to assimilate suitable actions, progressively adapt, acquire new skills, and engage in trial-and-error experiences. Noteworthy components of RL include the agent's adeptness at interacting with the environment and information gathering, without necessitating an exhaustive understanding or control over the environment [18].

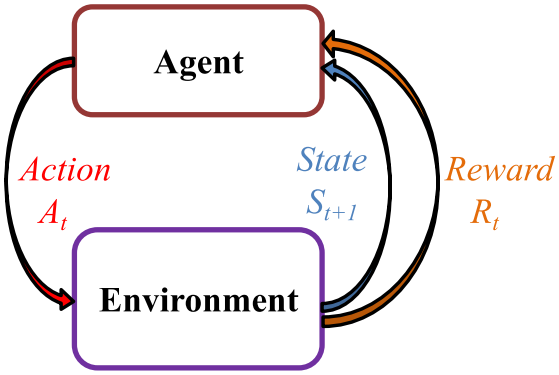

FIGURE 2. Main block diagram of the process of a generic RL system.

1) TRAINING ALGORITHM

The RL structure is framed as a discrete-time stochastic control process. This process involves an agent engaging with its environment within the context of a discrete-time Markov Decision Process (MDP).

Specifically, a discrete-time MDP is described by the tuple (S, A, p, R) where S is the environment state set, A is the system action set, p is the state transition probability and R is the reward function. More precisely, the state transition probability (p) is the probability of transition from the current state $s_t \in S$ at time t to state $s_{t+1} \in S$ at time $t+1$ under action $a \in A$:

$$p : S \times A \times S \rightarrow [0, 1]. \tag{15}$$

Moreover, the reward function R gives the reward after transition from s_t to s_{t+1} with action a:

$$R : S \times A \rightarrow [r_{min}, r_{max}]. \tag{16}$$

The objective in RL is that the agent obtains an optimal policy $\pi(s)$ (conditioning the action to be chosen in state s) that maximizes the reward function. The RL can directly calculate the optimal strategy without model knowledge and using a Q-function (Q-learning algorithm).

The Q-function, denoted as $Q(s,a)$ is a function that maps a state-action pair (s,a) to a value, representing the expected cumulative reward obtained by taking action a from state s and then following a certain policy. In this work, the selected agent is the Deep Deterministic Policy Gradient (DDPG) algorithm, a Q-learning actor-critic approach that consists of two parts: the actors that refers to a policy and the critic that estimates the Q-function. In the DDPG algorithm, both the actor and the Q-function (the critic) are approximated using

neural networks. These kind of agents are specially suitable for large continuous action spaces [53]. The used procedure is based on the steps described in the following.

1. Initialize the critic $Q(s,a)$ and target critic $Q_t(s,a)$ with the same random values of parameters (ϕ, ϕ_t).
2. Initialize the actor $\pi(s;\theta)$ and the target actor $\pi_t(s;\theta)$ with same random parameters (θ, θ_t).
3. For each episode:
   - 3.1 For the current state (s) of the episode select an action according to the policy $\pi(s;\theta) + N$, where N is configured as an exploration stochastic noise.
   - 3.2 Execute action (a) and observe the reward (r) and the next state (s').
   - 3.3 Store the experiences (s_i, a_i, r_i, s_i') in the experience buffer along a mini-batch of size M experiences.
   - 3.4 At each step of the training process, the parameters of the critic (ϕ) are updated. The update is made by minimizing the loss L_{critic} across sampled experiences of the mini-batch.

$$L_{critic} = \frac{1}{2M}\sum_{i=1}^{M}(y_i - Q(s_i,a_i;\phi)^2, \tag{17}$$

where a_i is the bounded action derived from the policy unbounded output from the actor $\pi(s_i;\theta)$. If s_i is a terminal state (final of the episode), the value function target (y_i) is exactly the experience reward r_i. If is not a terminal state, the value function target is the sum of r_i, and the discounted future reward (r') from the target critics considering the noise added by the agent.

$$y_i = r_i + \gamma * Q_t\left(s_i', \pi_t\left(s_i';\theta_t\right);\phi_t\right), \tag{18}$$

where the discount factor (γ) is an hyperparameter that represents how important are the nearest rewards over future rewards in perspective. To calculate the cumulative reward, the agent initiates the computation by determining the subsequent action. This is achieved by forwarding the next observation, s_i', obtained from the sampled experience to the target actor.

Depending on every time steps defined on the "*Policy frequency update*" hyperparameter, the parameters of the actor (θ) are updated by the policy gradient function searching to maximize the reward :

$$\nabla\theta J_{actor} \approx \frac{1}{M}\sum_{i=1}^{M}\left[\nabla A Q\left(s_i,a_i;\phi\right) * \nabla\theta\pi\left(s_i;\theta\right)\right] \tag{19}$$

where the first term of the product is the gradient of the output of the critic according to the action computed by the actor, and the second term is the gradient of output of the actor with respect to the actor parameters.

- 3.5 Update the target critic (Q_t) parameters (ϕ_t) and the target actor parameters (θ_t) with the hyperparameter called "*smooth factor*" (τ) following:

$$\phi_t = \tau\phi + (1-\tau)\,\phi_t \tag{20}$$

$$\theta_t = \tau\theta + (1-\tau)\,\theta_t. \tag{21}$$

The training algorithm is expressed in pseudocode in **Algorithm 1**.

Algorithm 1 DDPG Training Process

Input: ϕ, θ *and* M	•Initial parameters
$\phi_t \leftarrow \phi$	•Initialize target critic parameters with the critic parameters
$M \leftarrow \emptyset$	•Initialize the empty mini-batch M of buffer experiences
for each episode **do**	
for each environment step **do**	
$a_i \sim \pi(s;\theta) + N$	•Sample action from the policy adding exploration noise
$s_i' \sim p(s_i'\|s_i, a_i\|)$	•Sample state from the environment
$M \leftarrow \cup\left\{\left(s_i, a_i', r_i, s_i'\right)\right\}$	•Store the state in the mini-batch of buffer experiences
$\phi \leftarrow \phi$ -L_{critic} equation (17)	•Update the Q-function (critic) parameters
end for	
for each policy update step **do**	
$\theta \leftarrow \theta$ -$\nabla\theta J_{actor}$ equation (19)	•Update the policy parameters (actor)
$\phi \leftarrow \phi - \tau\phi + (1-\tau)\,\phi_t$	•Update target critic parameters
$\theta_t \leftarrow \theta_t - \tau\theta + (1-\tau)\,\theta_t$	•Update target actor parameters
end for	
end for	end of the episode
Output: ϕ, ϕ_t, θ	•Optimized parameters

III. CASE STUDY: SCNB WITH ANC SYSTEM

A. FINITE DIFFERENCE TIME DOMAIN ENVIRONMENT

The FDTD environment follows the process outlined in Fig. 2. By utilizing time-domain simulation techniques like FDTD, RL can interact in real-time throughout the optimization process, enabling adjustments to be made at each time step. On the contrary, the standard frequency-domain

simulation techniques only allow optimization after the process has finished and the stationary study returns the results.

Fig. 3 provides an overview of the simulation environment. The primary noise source is a moving car that emits a sinusoidal pure tone. The car travels from the lower to the upper boundary of the environment at a speed of 100 km/h. Each time the car passes through, it varies the frequency of the emitted tone, selecting a different random frequency ranging from 100 to 500 Hz. These frequencies represent the low range of the traffic noise spectrum, where the SCNB is almost transparent. The noise produced by the passing vehicle is measured at a reference point. The recorded signal is then processed and broadcasted from a secondary source to enhance noise mitigation at the evaluation point, combining the properties of the SCNB and the Active Noise Control (ANC) system. During the assessment phase, the cancellation signal from the loudspeaker and the car noise are evaluated to achieve noise cancellation following the principles of ANC. The FDTD simulation is conducted within a distinct function that the agent activates whenever it intends to interact with the environment. Consequently, this environment accepts inputs such as agent actions to be taken during the duration of time steps and provides outputs in the form of states or observations. Absorbing boundary conditions are implemented at the model's boundaries to mimic an open-field situation, following the form of Perfectly Matched Layers (PMLs) [49]. The code of the FDTD simulations has been developed entirely by the authors of this paper following the equations of section II-A. We wrote it with MATLAB, but FDTD is not a method native to that language, so that means that it would be possible to implement it with a variety of different programming languages.

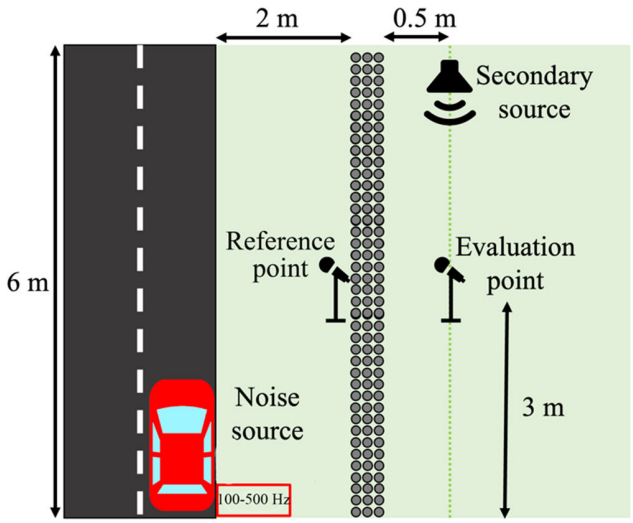

FIGURE 3. The FDTD Environment of the SCNB with the ANC system.

B. STATES

The primary objective of the RL architecture is to enhance the efficiency of the SCNB when coupled with the ANC system. Initially, the acoustic insulation provided solely by the barrier is considered as the baseline for reducing the acoustic pressure level. This serves as the initial observation in the process, i.e., the reset function of each episode. Following the execution of actions, a secondary pressure level is recorded, and subsequently, the Insertion Loss of the ANC system (IL_{ANC}) is computed according to the following formulation:

$$IL_{ANC} = 20 \times log_{10}\left(\frac{\sum_{t}^{t_{maxStep}} p\,(t)_b}{\sum_{t}^{t_{maxStep}} p\,(t)_{ANC}}\right), \qquad (22)$$

where numerator comes from the reset function of each frequency when the ANC system is off, being $p\,(t)_b$ the pressure measured only having the SCNB without the ANC working. The denominator is the result of each step function when the ANC system is working. That implies that at each step of the episode, the state is measured as $p\,(t)_{ANC}$ at the evaluation point. The whole episode of a car passing is equally divided in 5 steps, with $t_{maxStep} \cong 30$ ms. IL_{ANC} is calculated at each step of the episode, having the summatory in the first step only one value, and at the end of the episode 5 values.

C. ACTIONS

The actions space is continuous, and it has two different actions that can be explored in the RL system to modify the signal emitted by the secondary source. Both actions aim to generate an optimal signal capable of canceling the noise emanating from the noise source (car). But when the reference microphone (reference point) registers a pressure with the auditability threshold ($2{\cdot}10^{-5}$ Pa), the secondary source filters the sinusoidal signal from the car and starts emitting from the secondary source. The first action (action 1) determines the amplitude level of the signal emitted by the source, while the second action (action 2) determines the phase of the signal. The range of $Action_1$ is from 0 to 0.5 Pa, and $Action_2$ has a range of variation between 0 and $2\,\pi$.

When the phases of the signals are in opposition, the acoustic wave is canceled, creating a 'sweet point' in accordance with the main principle of ANC. The signal of the secondary source ($S2$) is described by the following equation:

$$S2 = -Action_1 \times sin\,(2\pi ft + Action_2)\,, \qquad (23)$$

with f being the random frequency from the car settled in the reset function and measured at the reference point. As previously explained, an episode is defined when the car is passing through the whole environment, and 5 actions pairs are applied to every episode as there are 5 times steps and two actions in the action set to cancel the noise from the car.

D. REWARD

The agent executes its behavior during each invocation of the step function, defined at intervals of $t_{maxStep} \cong 30$ ms, and receives rewards based on how these actions influence the environment according to the states observed. The reward serves as feedback from the environment, indicating the success or failure of the agent's activities. The agent is tasked

with adjusting certain parameters of the signal emitted from the secondary source to optimize noise cancellation at the evaluation point. Building upon the observations previously detailed, the Reward function (R) evaluates the Insertion Loss of the ANC system (IL_{ANC}) and assigns its value proportionally based on the extent to which the insulation is improved:

$$R = \begin{cases} IL_{ANC}, & IL_{ANC} > 0 \\ 0, & IL_{ANC} < 0. \end{cases} \quad (24)$$

IV. RESULTS

This section presents the results obtained from the ANC system in the SCNB. More specifically, first the training process of the SAC agent is presented, then the validation with the trained agent is proposed and finally the analysis of the acoustic performance of the system is discussed.

A. TRAINING

During the process up to having a trained agent, the hyperparameters condition the process, and Table 2 shows all the values for the different parts of the RL system, the Critical and Actor networks.

TABLE 2. Hyperparameters DDPG.

Name	Value
Agent Batch size	512
Agent buffer length (number of samples)	$1{\cdot}10^5$
Agent smooth factor (τ)	0.001
Agent Discount factor (γ)	0.99
Target Update frequency	1
Target smooth factor	0.001
Actor Learn rate	0.001
Actor Optimizer type	adam
Critic Optimizer type	adam
Critic Optimizer learn rate	0.01

The hyperparameters were tuned after observing different training processes. In the following Fig. 4 the training process is presented.

The black dots shown in Fig. 4 a) represents the different random frequencies between 100 and 500 Hz during the training process. The total accumulated rewards throughout the training phase can be observed in Fig. 4 b). The cumulative reward for each episode is depicted in blue, while the overall average reward is highlighted in red. Even if the average reward is not very high compared to the single one obtained at some frequencies, it is still an improvement compared with the no ANC system case. Since the reward function was chosen to only be positive if the IL_{ANC} is better than the Insertion Loss produced with the SCNB and without ANC system (IL).

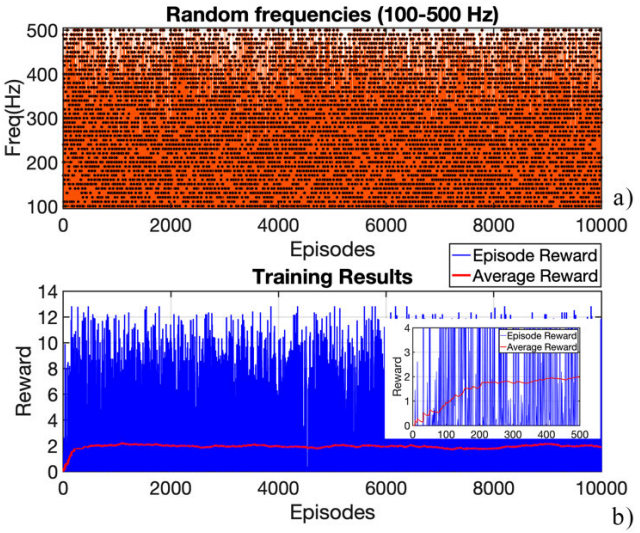

FIGURE 4. Training results of the DDPG agent. random frequencies of each episode a). Episode rewards (blue) and the cumulative average reward of all episodes(red) b).

At some frequencies, the system improved the insulation up to 40 dB according to equation 22. That value represents the cumulative reward so it can be deduced that, taking into account that there are 5 steps, about 5 dB in average is obtained with ANC SCNB while the vehicle is passing by.

B. DEPLOYMENT

Following the completion of training, the agent was considered for testing in the ANC procedure, aimed at assessing its capacity to respond to various frequencies, to be contrasted with the non-trained configuration. Additionally, the agent underwent testing to evaluate its performance against different car velocities, accounting for adjustments due to the Doppler effect. Differing from its training conditions, when only a velocity of 100 km/h was considered.

Despite being trained with random frequencies ranging from 100 to 500 Hz with the car (acting as a moving source) passing at 100 km/h, the agent demonstrated slightly diminished rewards when modifying the car velocity. Fig. 5 illustrates 21 distinct deployment episodes within the low-frequency range of interest (100-500 Hz) with a frequency step size of 20 Hz. Three velocities were examined: 100 km/h, which was utilized during the training phase, and 110 km/h and 120 km/h as additional velocities and new deployment scenarios.

In deployment scenarios, the agent faces additional real-world conditions beyond its training environment, such as varying car velocities. This testing phase is crucial for evaluating the agent's adaptability and generalization capabilities.

It is noted that the non-trained agent (see Fig. 5a) achieved approximately 1 or 2 dB of improvement in certain instances, particularly within the lower frequency range (100-220 Hz). This improvement can be attributed to the agent's ability to

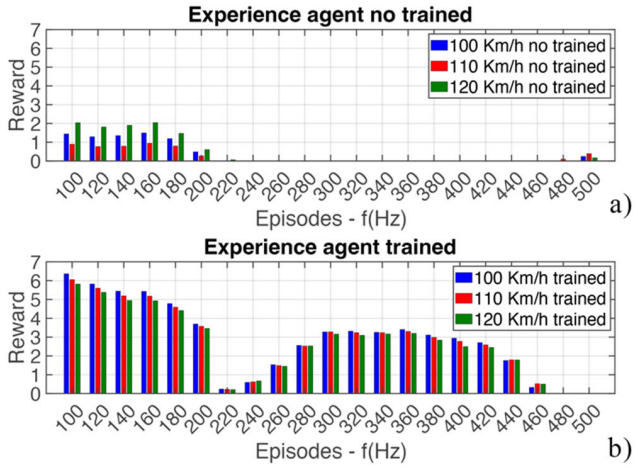

FIGURE 5. Comparison between DDPG agent deployment performance along 21 episodes (100-500 Hz range) with different car velocities before training the agent (a) and after training it (b).

take four additional actions during each frequency episode as per the initial step, aimed at enhancing performance. However, despite these efforts, the improvement obtained remains modest compared to the SCNB without ANC.

In contrast to that, the trained agent (see Fig. 5 ILb) obtains a remarkable improvement in the low frequencies and decreases with the frequency. Moreover, in the high frequency cases, the trained agent does not obtain an improvement compared to the SCNB without ANC. Hence, the lower the frequency is, the better performance of the cancellation principle of ANC works. The limit of the interest range of improvement is about 480 Hz, and even the agent has passed the training process, it was not possible to improve the SCNB with the ANC system.

The levels plotted are the average of the 5 steps of each episode, since each step was making a cumulative reward of all steps, bigger than the overall time calculation (about 40 dB) and the global vision of the insulation in dB is represented (around 4-5 dB in some cases).

The deployment scenarios highlight the challenges of real-world applications, where factors like varying car velocities can significantly impact the performance of the agent. Despite training in a controlled environment, the agent's effectiveness may vary when faced with these real-world complexities. Therefore, comprehensive testing under diverse conditions is essential to assess the agent's robustness and effectiveness in practical settings.

The insulation analysis with a global view depending on frequency spectrum is explained in the next section, together with the FDTD simulations results and the global acoustic performance.

C. ANALYSIS

Considering that noise at higher frequencies can be mitigated with absorbent materials or other complementary solutions to the SCNB mechanisms, the IL analysis is plotted only showing until 2 kHz. The SCNB has 3 rows and 27 columns, and the main insulation mechanism is designed to mainly mitigate at 1 kHz, considering the peak of traffic noise spectrum [37]. In Fig. 6 the Insertion Loss (IL) of the barrier is plotted without the ANC considering that the noise incidence is not normal, neither diffuse. The car is moving at 100, 110 and 120 km/h, which produces different angles of incidence of the sound during the time it travels through the FDTD domain. Usually, SCNB are studied at normal incidence as enlightened in introduction, some studies have also considered the diffuse incidence [46], but this approach looks for more realistic noise barrier case which is the moving source incidence. In blue, the insulation provided without the ANC is plotted until 2 kHz, to mainly observe where the SCNB produces bigger values due to its noise control phenomena [38]. For the three deployment scenarios under consideration (100, 110, and 120 km/h), represented by blue diamonds, red stars, and green stars respectively, the rewards obtained for each frequency with the trained agent (as depicted in Fig. 5b) are added to the original IL. In the low frequency range (100-500 Hz), the significant insulation improvement can be seen, and this is obtained without modifying the barrier. The IL shows in dB the difference between having the barrier or not and the noise reduction. At some frequencies, it has been seen that the ANC system is capable to produces bigger improvements (8 and 6 dB in the peaks), but the Fabry-Perot resonances are still present in the IL spectrum.

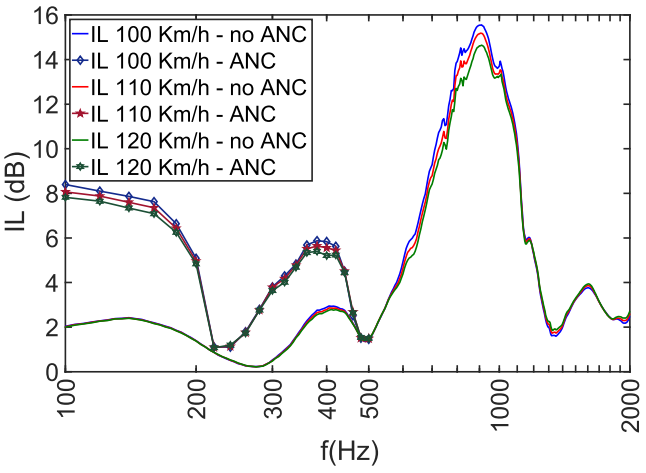

FIGURE 6. Insertion Loss of a SCNB of 3 rows with a moving source of 100, 110 and 120 Km/h incidence, with and without the ANC system working.

Finally, an instantaneous representation of the FDTD environment is showed in Fig. 7, where the ANC system is switched off in Fig. 7 a) and a small modulation of the 200 Hz noise wave is observed close to the reference microphone due to the SCNB. Fig. 7 b) shows the ANC working and producing interferences to mitigate the sound in the evaluation point. Considering that t = 0 ms is when the car is starting to move from the top at 100 Km/h, Fig. 7 represents the

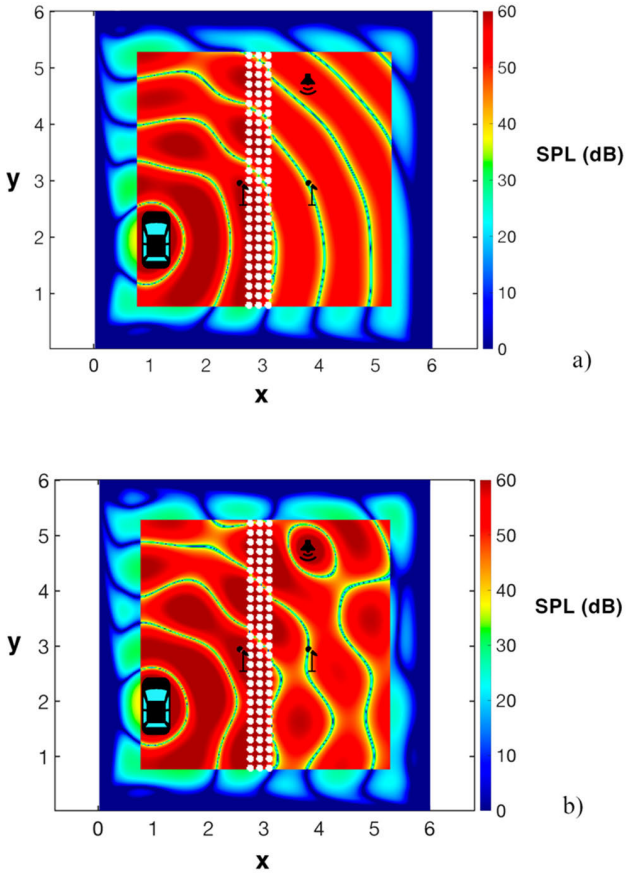

FIGURE 7. FDTD SPL maps at t = 30 ms with the car emitting noise at a frequency of 200 Hz. a) the ANC system switched off; b) the ANC system switched on.

instant of t = 30 ms, which is the moment after the first step function is executed and the first state is observed from the FDTD environment. The Sound Pressure Level (SPL) maps represent in dB the acoustic pressure distribution in the whole environment at that specific instant. The PMLs are working perfectly preventing reflections as in the deep blue color the 0 dB is obtained at the boundaries.

V. CONCLUSION

This work has presented a complete framework to smartly approach the issue of low frequency insulation on SCNB. Without modifying the geometry of the barrier or increasing the width, the placement of an ANC system improves the insulation in the lower frequency range of traffic noise spectrum (100-500 Hz) [54]. The use of FDTD numerical simulations extendedly validated in other works previously mentioned, allows the fast calculation of RL steps, and the quick modification of the cancelling secondary source parameters. The case of road traffic noise produced by a mobile source is analyzed. This approach is more realistic than the assumption of normal or diffuse incidence. Since SCNB are designed to insulate specific target frequencies, the ability to address random noise frequencies with the RL system is one of the biggest milestones. Further analysis of doppler effects of the moving source and different locations of the secondary cancelling source will be forthcoming studies. In the future research lines, the search of very low latency systems will be performed to quickly modify the loudspeaker emission parameters and to properly mitigate the noise in an experimental validation. Also, the implementation of speakers in the last row of the scatterers of the SCNB will be consider, for the purpose to have a more compact system.

REFERENCES

[1] J. Zhang, B. Hu, and S. Wang, "Review and perspective on acoustic metamaterials: From fundamentals to applications," *Appl. Phys. Lett.*, vol. 123, no. 1, Jul. 2023, Art. no. 010502, doi: 10.1063/5.0152099.
[2] H. Xiang, X. Ma, and J. Xiang, "Optimization for a locally resonant phononic crystal of square spiral with circle inside," *IEEE Access*, vol. 7, pp. 145988–145995, 2019, doi: 10.1109/ACCESS.2019.2946085.
[3] S. Tang, R. Wang, and J. Han, "Directional transmission characteristics of acoustic waves based on artificial periodic structures," *IEEE Access*, vol. 7, pp. 94033–94038, 2019, doi: 10.1109/ACCESS.2019.2928988.
[4] J. V. Sanchez-Perez, C. Rubio, R. Martinez-Sala, R. Sanchez-Grandia, and V. Gomez, "Acoustic barriers based on periodic arrays of scatterers," *Appl. Phys. Lett.*, vol. 81, no. 27, pp. 5240–5242, Dec. 2002, doi: 10.1063/1.1533112.
[5] Z. Maekawa, "Noise reduction by screens," *Appl. Acoust.*, vol. 1, no. 3, pp. 157–173, Jul. 1968, doi: 10.1016/0003-682x(68)90020-0.
[6] C. M. Harris, *Handbook of Acoustical Measurements and Noise Control*. New York, NY, USA: McGraw-Hill, 1991, pp. 3019–3020.
[7] L. Fredianelli, L. Del Pizzo, and G. Licitra, "Recent developments in sonic crystals as barriers for road traffic noise mitigation," *Environments*, vol. 6, no. 2, p. 14, Jan. 2019, doi: 10.3390/environments6020014.
[8] S. M. Kuo and D. R. Morgan, "Active noise control: A tutorial review," *Proc. IEEE*, vol. 87, no. 6, pp. 943–975, Jun. 1999, doi: 10.1109/5.763310.
[9] S. Kim and M. E. Altinsoy, "Comprehensive active control of booming noise inside a vehicle caused by the engine and the driveline," *IEEE Access*, vol. 10, pp. 49725–49737, 2022, doi: 10.1109/ACCESS.2022.3172969.
[10] F. Mori, A. Santoni, P. Fausti, F. Pompoli, P. Bonfiglio, and P. Nataletti, "The effectiveness of least mean squared-based adaptive algorithms for active noise control system in a small confined space," *Appl. Sci.*, vol. 13, no. 20, p. 11173, Oct. 2023, doi: 10.3390/app132011173.
[11] G. Lu, R. Chen, and H. Liu, "Active noise control scheme for smart beds based on a wide and narrow band hybrid control algorithm," *IEEE Access*, vol. 11, pp. 92617–92627, 2023, doi: 10.1109/ACCESS.2023.3308694.
[12] F. Jabeen, A. Mirza, A. Zeb, M. Imran, F. Afzal, and A. Maqbool, "FxRLS algorithms based active control of impulsive noise with online secondary path modeling," *IEEE Access*, vol. 9, pp. 117471–117485, 2021, doi: 10.1109/ACCESS.2021.3105902.
[13] S. Ise, H. Yano, and H. Tachibana, "Basic study on active noise barrier.," *J. Acoust. Soc. Jpn. E*, vol. 12, no. 6, pp. 299–306, 1991, doi: 10.1250/ast.12.299.
[14] S. Sohrabi, T. P. Gómez, and J. R. Garbí, "Suitability of active noise barriers for construction sites," *Appl. Sci.*, vol. 10, no. 18, p. 6160, Sep. 2020, doi: 10.3390/app10186160.
[15] J. Guo and J. Pan, "Increasing the insertion loss of noise barriers using an active-control system," *J. Acoust. Soc. Amer.*, vol. 104, no. 6, pp. 3408–3416, Dec. 1998, doi: 10.1121/1.423924.
[16] W. Chen, W. Rao, H. Min, and X. Qiu, "An active noise barrier with unidirectional secondary sources," *Appl. Acoust.*, vol. 72, no. 12, pp. 969–974, Dec. 2011., doi: 10.1016/j.apacoust.2011.06.006.
[17] R. S. Sutton and A. Barto, *Reinforcement Learning: An Introduction* (Adaptive Computation and Machine Learning), 2nd ed. Cambridge, MA, USA: MIT Press, 2020.
[18] V. Francois-Lavet, P. Henderson, R. Islam, M. G. Bellemare, and J. Pineau, "An introduction to deep reinforcement learning," 2018, *arXiv:1811.12560*.
[19] G. Volpe, A. M. Mangini, and M. P. Fanti, "A deep reinforcement learning approach for competitive task assignment in enterprise blockchain," *IEEE Access*, vol. 11, pp. 48236–48247, 2023, doi: 10.1109/ACCESS.2023.3276859.

[20] F. Parisi, V. Sangiorgio, N. Parisi, A. M. Mangini, M. P. Fanti, and J. M. Adam, "A new concept for large additive manufacturing in construction: Tower crane-based 3D printing controlled by deep reinforcement learning," *Construction Innov.*, vol. 24, no. 1, pp. 8–32, Jan. 2023, doi: 10.1108/ci-10-2022-0278.

[21] B. Raeisy, S. Golbahar Haghighi, and A. A. Safavi, "Active noise control system via multi-agent credit assignment," *J. Intell. Fuzzy Syst.*, vol. 26, no. 2, pp. 1051–1063, 2014, doi: 10.3233/ifs-130797.

[22] S. A. Hoseini Sabzevari and M. Moavenian, "Application of reinforcement learning for active noise control," *Turk J. Elec. Eng. Comp. Sci.*, vol. 25, no. 4, pp. 2606–2613, 2017, doi: 10.3906/elk-1602-189.

[23] Y.-J. Guan, Y. Ge, H.-X. Sun, S.-Q. Yuan, and X.-J. Liu, "Low-frequency, open, sound-insulation barrier by two oppositely oriented Helmholtz resonators," *Micromachines*, vol. 12, no. 12, p. 1544, Dec. 2021, doi: 10.3390/mi12121544.

[24] M. P. Peiró-Torres, M. Ferri, L. M. Godinho, P. Amado-Mendes, F. Jose Vea Folch, and J. Redondo, "Normal incidence sound insulation provided by Sonic Crystal Acoustic Screens made from rigid scatterers—assessment of different simulation methods," *Acta Acust.*, vol. 5, no. 28, 2021, doi: 10.1051/aacus/2021021.

[25] D. Ramírez-Solana, J. Redondo, A. M. Mangini, and M. P. Fanti, "Particle swarm optimization of resonant sonic crystals noise barriers," *IEEE Access*, vol. 11, pp. 38426–38435, 2023, doi: 10.1109/ACCESS.2023.3267972.

[26] F. Aslan and R. Paurobally, "Modelling and simulation of active noise control in a small room," *J. Vib. Control*, vol. 24, no. 3, pp. 607–618, Feb. 2018, doi: 10.1177/1077546316647572.

[27] K. Yee, "Numerical solution of initial boundary value problems involving Maxwell's equations in isotropic media," *IEEE Trans. Antennas Propag.*, vol. AP-14, no. 3, pp. 302–307, May 1966, doi: 10.1109/TAP.1966.1138693.

[28] J. Redondo, R. Picó, M. R. Avis, and T. J. Cox, "Prediction of the random-incidence scattering coefficient using a FDTD scheme," *Acta Acustica United Acustica*, vol. 95, no. 6, pp. 1040–1047, Nov. 2009, doi: 10.3813/aaa.918236.

[29] J. Redondo, R. Picó, V. J. Sánchez-Morcillo, and W. Woszczyk, "Sound diffusers based on sonic crystals," *J. Acoust. Soc. Amer.*, vol. 134, no. 6, pp. 4412–4417, Dec. 2013, doi: 10.1121/1.4828826.

[30] M. Cingolani, G. Fratoni, L. Barbaresi, D. D'Orazio, B. Hamilton, and M. Garai, "A trial acoustic improvement in a lecture Hall with MPP sound absorbers and FDTD acoustic simulations," *Appl. Sci.*, vol. 11, no. 6, p. 2445, Mar. 2021, doi: 10.3390/app11062445.

[31] T. Miyashita, "Sonic crystals and sonic wave-guides," *Meas. Sci. Technol.*, vol. 16, no. 5, pp. R47–R63, May 2005, doi: 10.1088/0957-0233/16/5/r01.

[32] J. Redondo, P. Gaja-Silvestre, L. Godinho, and P. Amado-Mendes, "A simple method to estimate the in situ performance of noise barriers," *Appl. Sci.*, vol. 12, no. 14, p. 7027, Jul. 2022, doi: 10.3390/app12147027.

[33] A. Kurowski and B. Kostek, "Reinforcement learning algorithm and FDTD-based simulation applied to schroeder diffuser design optimization," *IEEE Access*, vol. 9, pp. 136004–136017, 2021, doi: 10.1109/ACCESS.2021.3114628.

[34] W. W. Lang, G. C. Maling Jr., M. A. Nobile, R. E. Wise, and D. M. Yeager, "Design and performance of a hemi-anechoic room for measurement of the noise emitted by computer and business equipment," *Noise News Int.*, vol. 1, no. 1, pp. 1–60, Jan. 1993, doi: 10.3397/1.3702011.

[35] J. Sánchez-Dehesa, V. M. Garcia-Chocano, D. Torrent, F. Cervera, S. Cabrera, and F. Simon, "Noise control by sonic crystal barriers made of recycled materials," *J. Acoust. Soc. Amer.*, vol. 129, no. 3, pp. 1173–1183, Mar. 2011, doi: 10.1121/1.3531815.

[36] B. Raeisy, S. Golbahar Haghighi, and A. A. Safavi, "Active methods to control periodic acoustic disturbances invoking Q-learning techniques," *Nonlinear Dyn.*, vol. 74, no. 4, pp. 1317–1330, Dec. 2013, doi: 10.1007/s11071-013-1042-1.

[37] J. V. Sanchez-Perez, S. Castineira-Ibanez, V. Romero-Garcia, and L. M. Garcia-Raffi, "Periodic systems as road traffic noise reducing devices: Prototype and standardization," *Environ. Eng. Manage. J.*, vol. 14, no. 12, pp. 2759–2769, 2015, doi: 10.30638/eemj.2015.293.

[38] F. Morandi, M. Miniaci, A. Marzani, L. Barbaresi, and M. Garai, "Standardised acoustic characterisation of sonic crystals noise barriers: Sound insulation and reflection properties," *Appl. Acoust.*, vol. 114, pp. 294–306, Dec. 2016.

[39] C. Wang, Z. Wang, W. Sun, and D. R. Fuhrmann, "Reinforcement learning-based adaptive transmission in time-varying underwater acoustic channels," *IEEE Access*, vol. 6, pp. 2541–2558, 2018, doi: 10.1109/ACCESS.2017.2784239.

[40] K. Latifi, A. Kopitca, and Q. Zhou, "Model-free control for dynamic-field acoustic manipulation using reinforcement learning," *IEEE Access*, vol. 8, pp. 20597–20606, 2020, doi: 10.1109/ACCESS.2020.2969277.

[41] K. Mohapatra and D. P. Jena, "Insertion loss of sonic crystal made with multi resonant shells," *Appl. Acoust.*, vol. 171, Jan. 2021, Art. no. 107676, doi: 10.1016/j.apacoust.2020.107676.

[42] X. Qin, A. Ni, Z. Chen, M. Fang, and Y. Li, "Numerical modeling and field test of sonic crystal acoustic barriers," *Environ. Sci. Pollut. Res.*, vol. 30, no. 6, pp. 16289–16304, Oct. 2022, doi: 10.1007/s11356-022-23109-2.

[43] T. D'Orazio, F. Asdrubali, L. Godinho, M. Veloso, and P. Amado-Mendes, "Experimental and numerical analysis of wooden sonic crystals applied as noise barriers," *Environments*, vol. 10, no. 7, p. 116, Jul. 2023, doi: 10.3390/environments10070116.

[44] J. Redondo, D. Ramírez-Solana, and R. Picó, "Increasing the insertion loss of sonic crystal noise barriers with Helmholtz resonators," *Appl. Sci.*, vol. 13, no. 6, p. 3662, Mar. 2023, doi: 10.3390/app13063662.

[45] S. Sohrabi, T. P. Gómez, and J. R. Garbí, "Proper location of the transducers for an active noise barrier," *J. Vib. Control*, vol. 29, nos. 9–10, pp. 2290–2300, May 2023, doi: 10.1177/10775463221077490.

[46] D. Ramírez-Solana, V. Sangiorgio, N. Parisi, J. Redondo, A. M. Mangini, and M. P. Fanti, "Parametric design and assessment of 3D printable open noise barrier: Device customization to protect buildings from train brake noise," *J. Archit. Eng.*, vol. 30, no. 2, 2024, Art. no. 04024006, doi: 10.1061/JAEIED.AEENG-1605.

[47] J. Redondo, R. Picó, B. Roig, and M. R. Avis, "Time domain simulation of sound diffusers using finite-difference schemes," *Acta Acustica United Acustica*, vol. 93, no. 4, pp. 611–622, 2007.

[48] A. Taflove, S. C. Hagness, and M. Piket-May, "Computational electromagnetics: The finite-difference time-domain method," in *The Electrical Engineering Handbook*. Amsterdam, The Netherlands: Elsevier, 2005, pp. 629–670, doi: 10.1016/B978-012170960-0/50046-3.

[49] J.-P. Berenger, "A perfectly matched layer for the absorption of electromagnetic waves," *J. Comput. Phys.*, vol. 114, no. 2, pp. 185–200, Oct. 1994, doi: 10.1006/jcph.1994.1159.

[50] X. Yuan, D. Borup, J. W. Wiskin, M. Berggren, R. Eidens, and S. A. Johnson, "Formulation and validation of Berenger's PML absorbing boundary for the FDTD simulation of acoustic scattering," *IEEE Trans. Ultrason., Ferroelectr., Freq. Control*, vol. 44, no. 4, pp. 816–822, Jul. 1997, doi: 10.1109/58.655197.

[51] X. Yuan, D. Borup, J. Wiskin, M. Berggren, and S. A. Johnson, "Simulation of acoustic wave propagation in dispersive media with relaxation losses by using FDTD method with PML absorbing boundary condition," *IEEE Trans. Ultrason., Ferroelectr., Freq. Control*, vol. 46, no. 1, pp. 14–23, Jan. 1999, doi: 10.1109/58.741419.

[52] H. M. Yao and L. Jiang, "Enhanced PML based on the long short term memory network for the FDTD method," *IEEE Access*, vol. 8, pp. 21028–21035, 2020, doi: 10.1109/ACCESS.2020.2969569.

[53] T. P. Lillicrap, J. J. Hunt, A. Pritzel, N. Heess, T. Erez, Y. Tassa, D. Silver, and D. Wierstra, "Continuous control with deep reinforcement learning," 2015, *arXiv:1509.02971*.

[54] *Road Traffic Noise Reducing Devices—Test Method for Determining the Acoustic Performance—Part 3: Normalized Traffic Noise Spectrum*, Standard EN 1793-3:1998, Eur. Committee for Standardisation, Brussels, Belgium, 1793.

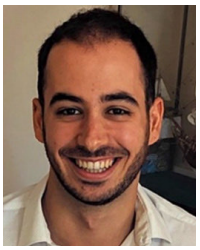

DAVID RAMÍREZ-SOLANA received the bachelor's degree in telecommunication engineering and the master's degree in acoustic from Universitat Politècnica de València (UPV). He is currently pursuing the dual Ph.D. degree in applied physics and electrical engineering with UPV and Politecnico di Bari. His research interests include acoustic metamaterials and their optimization, using new algorithms and techniques. Also, he is interested in simulation numerical methods for acoustics and the automation of noise mitigation devices, including active noise control strategies.

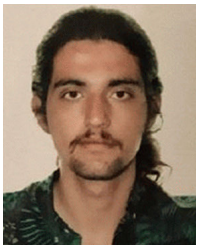

JAIME GALIANA-NIEVES received the bachelor's degree in telecommunications engineering with sound and image specialization from the University of Extremadura (UEx), in 2019, and the master's degree in acoustics engineering from the Polytechnic University of Valencia (UPV). He is currently pursuing the Ph.D. degree with special interest in wave propagation simulations, the application of genetic algorithms in the design of acoustic systems, and the study of time-varying metamaterials.

JAVIER REDONDO received the bachelor's degree in physics from the Autonomous University of Madrid, in 1993, the Ph.D. degree from the Quantum and Nonlinear Optics Research Group, University of Valencia, and the Ph.D. degree in acoustics from the Polytechnic University of Valencia (UPV), in 2001. He was an Assistant Professor with UPV. He has been a Visiting Professor with Université du Maine, France, and McGill University, Canada. He is currently a Full Professor of acoustics with UPV. He is also the Director of the Master's Degree in Acoustic Engineering, UPV, and a Local Coordinator of the Erasmus Mundus Joint Master's Degree WAVES (Waves, Acoustics, Vibrations, Engineering, and Sound). He is the coauthor of more than 40 articles in indexed scientific journals. His current research interests include simulation techniques in acoustics, room acoustics, building acoustics, metamaterials, and optimization using genetic algorithms.

AGOSTINO MARCELLO MANGINI (Senior Member, IEEE) received the Laurea degree in electronics engineering and the Ph.D. degree in electrical engineering from the Polytechnic University of Bari, Bari, Italy, in 2003 and 2008, respectively. He has been a Visiting Scholar with the University of Zaragoza, Zaragoza, Spain. He is currently an Associate Professor with the Department of Electrical and Information Engineering, Polytechnic University of Bari. He has authored or coauthored more than 130 printed publications. His current research interests include modeling, simulation, and control of discrete-event systems, Petri nets, supply chains and urban traffic networks, distribution and internal logistics, management of hazardous materials, management of drug distribution systems, and healthcare systems. He was on the Program Committees of the 2007–2015 IEEE International SMC Conference on Systems, Man, and Cybernetics, and the 2009 IFAC Workshop on Dependable Control of Discrete Systems. He was on the Editorial Board of the 2017 IEEE Conference on Automation Science and Engineering.

MARIA PIA FANTI (Fellow, IEEE) received the Laurea degree in electronic engineering from the University of Pisa, Pisa, Italy, in 1983. Since 1983, she has been with the Department of Electrical and Information Engineering, Polytechnic University of Bari, Italy, where she is currently a Full Professor of system and control engineering and the Chair of the Laboratory of Automation and Control. She was a Visiting Researcher with the Rensselaer Polytechnic Institute, Troy, NY, USA, in 1999. She has published more than 335 articles and two textbooks on her research topics. Her research interests include management and modeling of complex systems, such as transportation, logistics and manufacturing systems, discrete event systems, Petri nets, consensus protocols, and fault detection. She was a member of the Board of Governors of the IEEE Systems, Man, and Cybernetics Society and the AdCom of the IEEE Robotics and Automaton Society. She was the General Chair of the 2011 IEEE Conference on Automation Science and Engineering, the 2017 IEEE International Conference on Service Operations and Logistics, and Informatics, and the 2019 IEEE Systems, Man, and Cybernetics Conference. She is the Chair of the Technical Committee on Automation in Logistics of the IEEE Robotics and Automation Society. She is a Senior Editor of IEEE TRANSACTIONS ON AUTOMATION SCIENCE AND ENGINEERING and an Associate Editor of IEEE TRANSACTIONS ON SYSTEMS, MAN, AND CYBERNETICS: SYSTEMS.

Open Access funding provided by 'Politecnico di Bari' within the CRUI CARE Agreement